DEUTSCHES ELEKTRONEN-SYNCHROTRON

Ein Forschungszentrum der Helmholtz-Gemeinschaft

DESY 12-034

February 2012

Self-seeding scheme for the soft X-ray line at the European XFEL

Gianluca Geloni, European XFEL GmbH, Hamburg

Vitali Kocharyan and Evgeni Saldin Deutsches Elektronen-Synchrotron DESY, Hamburg

ISSN 0418-9833

NOTKESTRASSE 85 - 22607 HAMBURG

Self-seeding scheme for the soft X-ray line at the European XFEL

Gianluca Geloni,^{a,1} Vitali Kocharyan^b and Evgeni Saldin^b

^aEuropean XFEL GmbH, Hamburg, Germany ^bDeutsches Elektronen-Synchrotron (DESY), Hamburg, Germany

Abstract

This paper discusses the potential for enhancing the capabilities of the European FEL in the soft X-ray regime. A high longitudinal coherence will be the key to such performance upgrade. In order to reach this goal we study a very compact soft X-ray self-seeding scheme originally designed at SLAC [1, 2]. The scheme is based on a grating monochromator, and can be straightforwardly installed in the SASE3 undulator beamline at the European XFEL. For the European XFEL fully-coherent soft X-ray pulses are particularly valuable since they naturally support the extraction of more FEL power than at saturation by exploiting tapering in the tunable-gap SASE3 undulator. Tapering consists of a stepwise change of the undulator gap from segment to segment. Based on start-to-end simulations we show that soft X-ray FEL power reaches about 800 GW, that is about an order of magnitude higher than the SASE level at saturation (100 GW). The self-seeding setup studied in this work is extremely compact (about 5 m long), and cost-effective. This last characteristic may justify to consider it as a possible addition to the European XFEL capabilities from the very beginning of the operation phase.

1 Introduction

The quality of the output radiation of X-ray SASE FELs is far from ideal. SASE X-ray beams are characterized by nearly full transverse coherence but only limited longitudinal coherence [3]-[5]. However, many experiments require both transverse and longitudinal coherence. In principle, one can create a longitudinal coherent source by using a monochromator located in experimental hall, but this is often undesirable because of intensity losses.

¹ Corresponding Author. E-mail address: gianluca.geloni@xfel.eu

An important goal for any advanced XFEL facility is the production of X-ray radiation pulses with minimum allowed photon energy width for a given pulse length, that is Fourier-limited pulses. In this way, no monochromator is needed in the experimental hall. Self-seeding is a promising approach to significantly narrow the SASE bandwidth and to produce nearly transform-limited pulses [6]-[21]. Considerable effort has been invested in theoretical investigation and R&D at LCLS leading to this capability [22].

In general, a self-seeding setup consists of two undulators separated by a photon monochromator and an electron bypass, normally a four-dipole chicane. The two undulators are resonant to the same radiation wavelength. The SASE radiation generated by the first undulator passes through the narrow-band monochromator. A transform-limited pulse is created, which is used as a coherent seed in the second undulator. Chromatic dispersion effects in the bypass chicane smear out the microbunching in the electron bunch, produced by the SASE lasing in the first undulator. The electrons and the monochromatized photon beam are recombined at the entrance of the second undulator, and radiation is amplified by the electron bunch until saturation is reached. The required seed power at the beginning of the second undulator must dominate over the shot noise power within the gain bandpass, which is order of a kW in the soft X-ray range.

For soft X-ray self-seeding, a monochromator usually consists of a grating [6]. Recently, a very compact soft X-ray self-seeding scheme has appeared, based on a grating monochromator [1, 2]. The proposed monochromator is composed of only three mirrors and a rotational VLS grating. A preliminary design of the gratings adopts a constant focal-point mode in order to have fixed slit location. When tuning the photon energy in the range between 250 and 1000 eV, the variation in the optical delay is limited to 10% of the nominal value of 2.5 ps. A short magnetic chicane delays the electron bunch accordingly, so that the photon beam passing through the monochromator system recombines with the same electron bunch. The chicane provides a dispersion strength of about 2 mm in order to match the optical delay and also smears out the SASE microbunching generated in the first undulator.

In this article we study the performance of the above-described scheme for the European XFEL upgrade. The installation of the chicane does not perturb the undulator focusing system and allows for a safe return to the baseline mode of operation. The inclusion of a chicane is not expensive and may find many other applications [23, 24].

With the radiation beam monochromatized down to the Fourier transform limit, a variety of very different techniques leading to further improvement of the X-ray FEL performance become feasible. In particular, the most promising way to extract more FEL power than that at saturation is by ta-

self-seeded soft X-ray FEL with grating monochromator

baseline gap-tunable undulator SASE3 (21 cells)

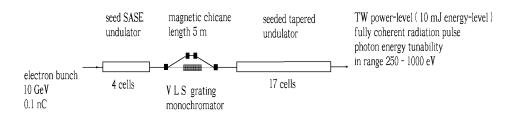


Fig. 1. Design of the self-seeding setup based on the European XFEL baseline undulator system for generating highly monochromatic, high power soft X-ray pulses. The method exploits a combination of a self-seeding scheme with a grating monochromator and of a undulator tapering technique. The self-seeding setup is composed of a compact (about 2.5 ps optical delay) grating monochromator originally proposed at SLAC [1, 2] and a 5 m-long magnetic chicane. The magnetic chicane accomplishes three tasks by itself. It creates an offset for monochromator installation, it removes the electron microbunching produced in the upstream (seed) undulator, and it acts as a electron beam delay line for monochromator optical delay compensation.

pering the magnetic field of the undulator [25]-[28]. A significant increase in power is achievable by starting the FEL process from monochromatic seed rather than from noise, [29]-[31]. In this paper we propose a study of the performance of the soft X-ray self-seeding scheme for the European XFEL, based on start-to-end simulations for an electron beam with 0.1 nC charge [32]. Simulations show that the FEL power of the transform-limited soft X-ray pulses may be increased up to 800 GW by properly tapering the baseline undulator. In particular, it is possible to create a source capable of delivering fully-coherent, 10 fs (FWHM) soft X-ray pulses with $0.6 \cdot 10^{14}$ photons per pulse at the wavelength of 1.5 nm.

2 Possible self-seeding scheme with grating monochromator for the baseline undulator SASE3

Any self-seeding setup should be compact enough to fit one undulator segment. The elements of the adopted electron bypass design are four 0.5 m-long dipole magnets of rectangular shape. Under the constraints imposed by space and strength of the magnetic field it is only possible to operate at an electron beam energy of 10 GeV. The first dipole deflects the beam by 1.25



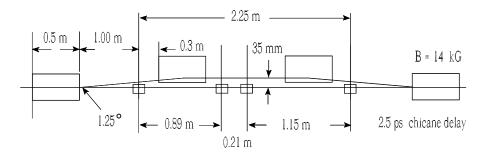


Fig. 2. Plan view of the self-seeding setup with compact grating monochromator originally proposed at SLAC [1, 2].

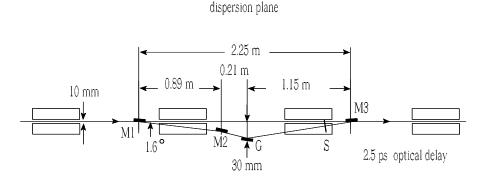


Fig. 3. Elevation view of the self-seeding setup with compact grating monochromator originally proposed at SLAC [1, 2].

degrees. After 1.8 m, the second dipole deflects the beam back in a direction parallel to the straight beampath at a distance of about 3 cm, which is sufficient for the installation of the optical elements of the monochromator. The total elongation of the electron beampath is approximately 1 mm. The layout of the bypass is shown in Fig. 2 and Fig. 3.

The monochromator design should be compact enough to fit with this magnetic chicane design. In particular, the optical delay should be matched to that induced by the magnetic chicane on the electron beam. The design adopted in this paper is the novel one by Y. Feng et al. [1, 2], and is based on a planar VLS grating. It is equipped only with an exit slit. Such design includes four optical elements, a cylindrical and spherical focusing mirrors, a VLS grating and a plane mirror in front of the grating. The specifications

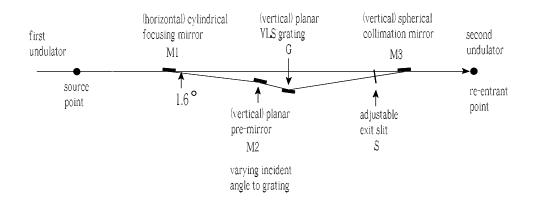


Fig. 4. Optics for the compact grating monochromator originally proposed at SLAC [1, 2] for the soft X-ray self-seeding setup.

of the monochromator are summarized below:

- The total optical beamline length, from the source to the image, is about 6 m.
- The total length between first and last optical components is about 2.3 m
- The delay of the photons is about 2.5 ps.
- The monochromator is continuously tunable in the photon energy range 250 1000 eV.
- The resolving power is about 4500 at the wavelength around 1.5 nm.
- The photon beam size and divergence at the entrance of the 2nd undulator are close to those at the exit of the first undulator.
- The transmission of the beamline is close to 10% for wavelengths around 1.5 nm.

The optical layout of the monochromator is schematically shown in Fig. 4. The first optical component in the monochromator, *M*1, is a cylindrical mirror which focuses the input photon beam in the sagittal plane at the entrance point, and deflects it in the dispersion plane of about 1.6 degree. This mirror has a long focal length of about 5 m. The last optical component, *M*3, is a collimation mirror that refocuses the photon beam at the entrance point. It introduces a deflection angle in the dispersion plane of about 1.2°. This mirror has a short focal distance of about 20 cm. The second mirror, *M*2, is plane mirror set in front of the grating. The function of this mirror is to illuminate the grating at the proper angle of incidence, which is chosen so that the correct wavelength is approximately focused at the exit slit. The monochromator scanning is performed by rotating and translating the premirror and by rotating the grating. The translation of the mirror implies that the optical path is wavelength dependent. Evidently, the scanning will result on a wavelength dependent optical path. The tunability of the path

	Units	
Undulator period	mm	65
Periods per cell	-	77
K parameter (rms)	-	4.2
Total number of cells	-	21
Intersection length	m	1.1
Wavelength	nm	1.5
Energy	GeV	10.0
Charge	nC	0.1

Table 1Parameters for the mode of operation at the European XFEL used in this paper.

length in the magnetic chicane will be required to compensate for the change in the optical path in the range of 0.1 mm. The last optical component is a planar VLS grating. A monochromator resolving power of about 4500 (at 1.5 nm) is obtained with the grating having a line spacing of 0.8 micron, a groove height of 11 nm and using a 3 microns exit slit [1, 2]. The estimated grating efficiency is about 10%. Reflectivity of the grazing incident mirrors and grating are close to 100%.

3 FEL simulations

With reference to Fig. 1, we performed a feasibility study with the help of the FEL code GENESIS 1.3 [33] running on a parallel machine. We will present a feasibility study for the SASE3 FEL line of the European XFEL, based on a statistical analysis consisting of 100 runs. The overall beam parameters used in the simulations are presented in Table 1.

The expected beam parameters at the entrance of the SASE3 undulator, and the resistive wake inside the undulator are shown in Fig. 5, [32]. The evolution of the transverse electron bunch dimensions are plotted in Fig. 6.

The SASE pulse power and spectrum after the first undulator in Fig. 1 is shown in Fig. 7. This pulse goes through the grating monochromator. We assume a monochromator with a Gaussian shape. At the exit of the monochromator, one obtains the seed pulse, Fig. 8. As explained before, the monochromator introduces only a short optical delay of about 2.5 ps, which can be easily compensated by the electron chicane. The chicane also washes out the electron beam microbunching. As a result, at the entrance of the second (output) undulator the electron beam and the radiation pulse can be

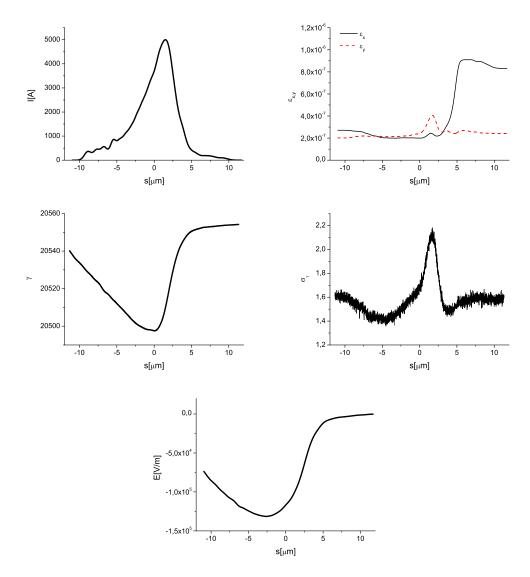


Fig. 5. Results from electron beam start-to-end simulations at the entrance of SASE3 [32]. (First Row, Left) Current profile. (First Row, Right) Normalized emittance as a function of the position inside the electron beam. (Second Row, Left) Energy profile along the beam. (Second Row, Right) Electron beam energy spread profile. (Bottom row) Resistive wakefields in the SASE3 undulator [32].

recombined.

If the output undulator is not tapered, one needs 7 sections to reach saturation. The best compromise between power and spectral bandwidth are reached after 6 sections, Fig. 9. In this case, the evolution of the energy per pulse and of the energy fluctuations as a function of the undulator length are shown in Fig. 10. The pulse now reaches the 100 GW power level, with an average relative FWHM spectral width narrower than 10^{-3} . Finally, the transverse radiation distribution and divergence at the exit of the output undulator are shown in Fig. 11.

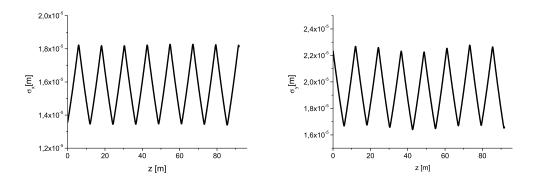


Fig. 6. Evolution of the horizontal (left plot) and vertical (right plot) dimensions of the electron bunch as a function of the distance inside the SASE3 undulator. The plots refer to the longitudinal position inside the bunch corresponding to the maximum current vale.

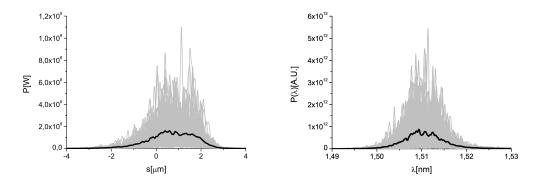


Fig. 7. Power distribution and spectrum of the X-ray radiation pulse after the first undulator. Grey lines refer to single shot realizations, the black line refers to the average over a hundred realizations.

The most promising way to increase the output power is via post-saturation tapering. Tapering consists in a slow reduction of the field strength of the undulator in order to preserve the resonance wavelength, while the kinetic energy of the electrons decreases due to the FEL process. The undulator taper could be simply implemented as a step taper from one undulator segment to the next, as shown in Fig. 12. The magnetic field tapering is provided by changing the undulator gap. A further increase in power is achievable by starting the FEL process from the monochromatic seed, rather than from noise. The reason is the higher degree of coherence of the radiation in the seed case, thus involving, with tapering, a larger portion of the bunch in the energy-wavelength synchronism. Using the tapering configuration in Fig. 12, one obtains the output characteristics, in terms of power and spectrum, shown in Fig. 13. The output power is increased of about a factor ten, allowing one to reach about one TW. The spectral width remains almost unvaried, with an average relative bandwidth (FWHM) narrower than 10^{-3} . The evolution of the energy per pulse and of the energy fluctuations as a

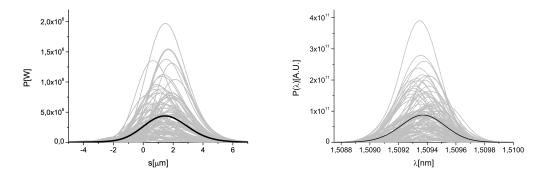


Fig. 8. Power distribution and spectrum of the X-ray radiation pulse after the monochromator. This pulse is used to seed the electron bunch at the entrance of the output undulator. Grey lines refer to single shot realizations, the black line refers to the average over a hundred realizations.

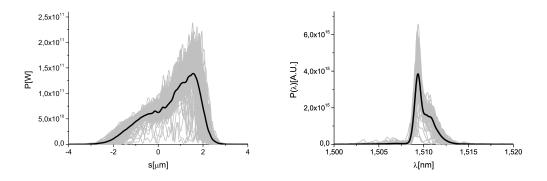


Fig. 9. Power distribution and spectrum of the X-ray radiation pulse after the second undulator in the untapered case. Grey lines refer to single shot realizations, the black line refers to the average over a hundred realizations.

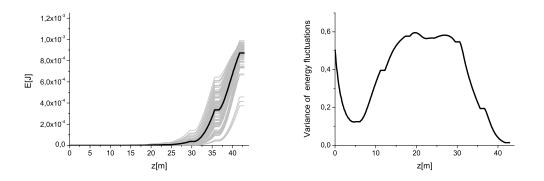


Fig. 10. Evolution of the energy per pulse and of the energy fluctuations as a function of the undulator length in the untapered case. Grey lines refer to single shot realizations, the black line refers to the average over a hundred realizations.

function of the undulator length are shown in Fig. 10. Finally, the transverse radiation distribution and divergence at the exit of the output undulator are

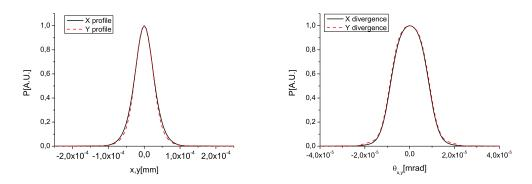


Fig. 11. (Left plot) Transverse radiation distribution in the untapered case at the exit of the output undulator. (Right plot) Directivity diagram of the radiation distribution in the case of tapering at the exit of the output undulator.

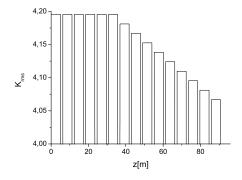


Fig. 12. Taper configuration for high-power mode of operation at 1.5 nm.

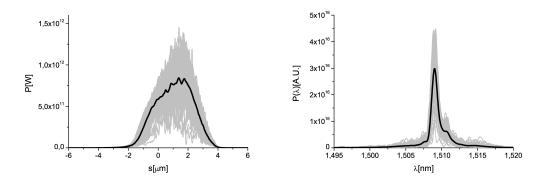


Fig. 13. Power distribution and spectrum of the X-ray radiation pulse after the second undulator in the tapered case. Grey lines refer to single shot realizations, the black line refers to the average over a hundred realizations.

shown in Fig. 15. By comparison with Fig. 11 one can see that the divergence decrease is accompanied by an increase in the transverse size of the radiation spot at the exit of the undulator.

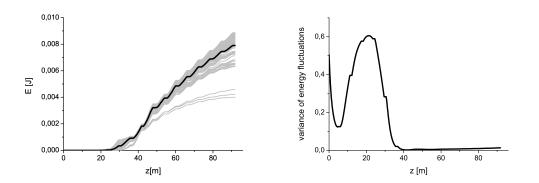


Fig. 14. Evolution of the energy per pulse and of the energy fluctuations as a function of the undulator length in the tapered case. Grey lines refer to single shot realizations, the black line refers to the average over a hundred realizations.

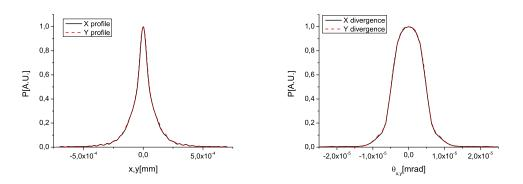


Fig. 15. (Left plot) Transverse radiation distribution in the case of tapering at the exit of the output undulator. (Right plot) Directivity diagram of the radiation distribution in the case of tapering at the exit of the output undulator.

4 Conclusions

In this paper we showed that monochromatization of soft X-ray pulses is of great importance for the European XFEL upgrade program. In fact, aside for an improvement of the longitudinal coherence, highly monochromatized pulses open up many possibilities to enhance the capacity of the European XFEL.

In particular we showed that monochromatization effectively allows one to use undulator tapering techniques enabling a TW-power mode of operation in the soft X-ray wavelength regime.

The progress which can be achieved with the methods considered here is based on the novel soft X-ray self-seeding scheme with grating monochromator [1, 2], which is extremely compact and can be straightforwardly realized at the European XFEL baseline undulator SASE3. Preliminary estimates seem to indicate that a monochromator efficiency close to 10% can be achieved. However, detailed efficiency calculations are required to determine if this is indeed the case. Another problem with the operation of this scheme can be the mismatching of the seed radiation pulse with the electron bunch. However, the safety margin of the proposed design is large enough: even if the nominal seed power (200 kW) is degraded of an order of magnitude due to non-ideal effects, one would still obtain a reasonable seed signal (20 kW) compared to the equivalent shot noise power (1 kW).

5 Acknowledgements

We are grateful to Massimo Altarelli, Reinhard Brinkmann, Serguei Molodtsov and Edgar Weckert for their support and their interest during the compilation of this work.

References

- [1] Y. Feng, J. Hastings, P. Heimann, M. Rowen, J. Krzywinski, and J. Wu, "X-ray Optics for soft X-ray self-seeding the LCLS-II", proceedings of 2010 FEL conference, Malmo, Sweden, (2010).
- [2] Y. Feng, P. Heimann, J. Wu, J. Krzywinski, M. Rowen, and J. Hastings, "Compact Grating Monochromator Design for LCLS-I Soft X-ray Self-Seeding", https://slacportal.slac.stanford.edu/ sites/lcls_public/lcls_ii/Lists/LCLS_II_Calendar/Physics_Meetings.aspx, May 2011 and https://sites.google.com/a/lbl.gov/realizing-thepotential-of-seeded-fels-in-the-soft-x-ray-regime-workshop/talks, October 2011
- [3] P. Emma et al., Nature photonics doi:10.1038/nphoton.2010.176 (2010)
- [4] T. Tanaka et al. (Eds.) Spring-8 Compact SASE Source (See Conceptual Design Kouto (2005)also report, http://www-xfel.spring8.or.jp/SCSSCDR.pdf)
- [5] M. Altarelli, et al. (Eds.) XFEL, The European X-ray Free-Electron Laser, Technical Design Report, DESY 2006-097, Hamburg (2006).
- [6] J. Feldhaus et al., Optics. Comm. 140, 341 (1997).
- [7] E. Saldin, E. Schneidmiller, Yu. Shvyd'ko and M. Yurkov, NIM A 475 357 (2001).
- [8] E. Saldin, E. Schneidmiller and M. Yurkov, NIM A 445 178 (2000).
- [9] R. Treusch, W. Brefeld, J. Feldhaus and U Hahn, Ann. report 2001 "The seeding project for the FEL in TTF phase II" (2001).
- [10] A. Marinelli et al., Comparison of HGHG and Self Seeded Scheme for the Production of Narrow Bandwidth FEL Radiation, Proceedings of FEL 2008, MOPPH009, Gyeongju (2008).

- [11] G. Geloni, V. Kocharyan and E. Saldin, "Scheme for generation of highly monochromatic X-rays from a baseline XFEL undulator", DESY 10-033 (2010).
- [12] Y. Ding, Z. Huang and R. Ruth, Phys.Rev.ST Accel.Beams, vol. 13, p. 060703 (2010).
- [13] G. Geloni, V. Kocharyan and E. Saldin, "A simple method for controlling the line width of SASE X-ray FELs", DESY 10-053 (2010).
- [14] G. Geloni, V. Kocharyan and E. Saldin, "A Cascade self-seeding scheme with wake monochromator for narrow-bandwidth X-ray FELs", DESY 10-080 (2010).
- [15] Geloni, G., Kocharyan, V., and Saldin, E., "Cost-effective way to enhance the capabilities of the LCLS baseline", DESY 10-133 (2010).
- [16] Geloni, G., Kocharyan V., and Saldin, E., "A novel Selfseeding scheme for hard X-ray FELs", Journal of Modern Optics, DOI:10.1080/09500340.2011.586473
- [17] J. Wu et al., "Staged self-seeding scheme for narrow bandwidth, ultrashort X-ray harmonic generation free electron laser at LCLS", proceedings of 2010 FEL conference, Malmo, Sweden, (2010).
- [18] G. Geloni, V. Kocharyan and E. Saldin, "Scheme for generation of fully coherent, TW power level hard x-ray pulses from baseline undulators at the European XFEL", DESY 10-108 (2010).
- [19] Geloni, G., Kocharyan, V., and Saldin, E., "Production of transformlimited X-ray pulses through self-seeding at the European X-ray FEL", DESY 11-165 (2011).
- [20] W.M. Fawley et al., Toward TW-level LCLS radiation pulses, TUOA4, to appear in the FEL 2011 Conference proceedings, Shanghai, China, 2011
- [21] J. Wu et al., Simulation of the Hard X-ray Self-seeding FEL at LCLS, MOPB09, to appear in the FEL 2011 Conference proceedings, Shanghai, China, 2011
- [22] The LCLS-II Conceptual design report, https://slacportal.slac.stanford. edu/sites/lcls_public/lcls_ii/Published_Documents/CDR%20Index.pdf
- [23] G. Geloni, V. Kocharyan and E. Saldin, "Ultrafast X-ray pulse measurement method", http://arxiv.org/abs/1001.3544 , DESY 10-008 (2010).
- [24] G. Geloni, V. Kocharyan and E. Saldin, "Scheme for femtosecondresolution pump-probe experiments at XFELs with two-color ten GWlevel X-ray pulses", http://arxiv.org/abs/1001.3510, DESY 10-004 (2010).
- [25] A. Lin and J.M. Dawson, Phys. Rev. Lett. 42 1670 (1979)
- [26] P. Sprangle, C.M. Tang and W.M. Manheimer, Phys. Rev. Lett. 43 1932 (1979)
- [27] N.M. Kroll, P. Morton and M.N. Rosenbluth, IEEE J. Quantum Electron., QE-17, 1436 (1981)
- [28] T.J. Orzechovski et al., Phys. Rev. Lett. 57, 2172 (1986)
- [29] W. Fawley et al., NIM A 483 (2002) p 537
- [30] M. Cornacchia et al., J. Synchrotron rad. (2004) 11, 227-238

- [31] X. Wang et al., PRL 103, 154801 (2009)
- [32] I. Zagorodnov, "Beam Dynamics Simulations for XFEL", http://www.desy.de/xfel-beam/s2e (2011).
- [33] S Reiche et al., Nucl. Instr. and Meth. A 429, 243 (1999).